Neurotherapeutics (2021) 18:2436–2448
https://doi.org/10.1007/s13311-021-01158-8

ORIGINAL ARTICLE

A Compound Mitigates Cancer Pain and Chemotherapy-Induced Neuropathic Pain by Dually Targeting nNOS-PSD-95 Interaction and $GABA_A$ Receptor

Wei Wei[1] · Weili Liu[1] · Shibin Du[1] · Gokulapriya Govindarajalu[1] · Antony Irungu[1] · Alex Bekker[1] · Yuan-Xiang Tao[1,2,3]

Accepted: 4 November 2021 / Published online: 18 November 2021

Abstract

Metastatic bone pain and chemotherapy-induced peripheral neuropathic pain are the most common clinical symptoms in cancer patients. The current clinical management of these two disorders is ineffective and/or produces severe side effects. The present study employed a dual-target compound named as ZL006-05 and examined the effect of systemic administration of ZL006-05 on RM-1–induced bone cancer pain and paclitaxel-induced neuropathic pain. Intravenous injection of ZL006-05 dose-dependently alleviated RM-1–induced mechanical allodynia, heat hyperalgesia, cold hyperalgesia, and spontaneously ongoing nociceptive responses during both induction and maintenance periods, without analgesic tolerance, affecting basal/acute pain and locomotor function. Similar behavioral results were observed in paclitaxel-induced neuropathic pain. This injection also decreased neuronal and astrocyte hyperactivities in the lumbar dorsal horn after RM-1 tibial inoculation or paclitaxel intraperitoneal injection. Mechanistically, intravenous injection of ZL006-05 potentiated the $GABA_A$ receptor agonist–evoked currents in the neurons of the dorsal horn and anterior cingulate cortex and also blocked the paclitaxel-induced increase in postsynaptic density-95–neuronal nitric oxide synthase interaction in dorsal horn. Our findings strongly suggest that ZL006-05 may be a new candidate for the management of cancer pain and chemotherapy-induced peripheral neuropathic pain.

Keywords ZL006-05 · Intravenous injection · PSD-95 · nNOS · $GABA_A$ receptor · Spinal cord dorsal horn · Anterior cingulate cortex · Metastatic bone cancer pain · Chemotherapy-induced neuropathic pain

Introduction

Intractable and persistent cancer pain is one of the most common clinical symptoms especially in the patients with bone metastasis [1, 2]. Chemotherapy-induced peripheral neuropathic pain (CIPNP) is also refractory and often causes a discontinuation of antineoplastic therapy and a decrease in survival rates of the patients [3, 4]. Cancer pain and CIPNP markedly impact quality of life, leading to significant socioeconomic burdens in the patients and their families [5]. Currently, several strategies including non-steroidal anti-inflammatory drugs, anticonvulsants, antidepressants, and opioids have been used in the managements of these two disorders. However, the majority of patients complain of unsatisfactory pain control and/or severe side effects such as nausea, dizziness, cognitive changes, cardiac arrhythmia, constipation, respiratory depression, opioid analgesic tolerance, and hyperalgesia [5]. Therefore, the development of novel analgesics is imperative in order to achieve ideal therapeutic efficacy in treatment of both cancer pain and CIPNP.

It is well documented that central sensitization in the central nervous system plays a key role in the genesis of chronic pain including cancer pain and CIPNP [6].

Wei Wei, Weili Liu, Shibin Du, and Gokulapriya Govindarajalu contributed equally to this work.

✉ Yuan-Xiang Tao
yuanxiang.tao@njms.rutgers.edu

[1] Department of Anesthesiology, Rutgers New Jersey Medical School, The State University of New Jersey, 185 S. Orange Ave., MSB, F-661, Newark, NJ 07103, USA

[2] Department of Physiology, Rutgers New Jersey Medical School, The State University of New Jersey, Pharmacology & Neuroscience, Newark, NJ 07103, USA

[3] Department of Cell Biology & Molecular Medicine, Rutgers New Jersey Medical School, The State University of New Jersey, Newark, NJ 07103, USA

NMDA receptors and their downstream signals (e.g., postsynaptic density protein-95 (PSD-95) or postsynaptic density protein-93 (PSD-93) and neuronal nitric oxide synthase (nNOS)) contribute to central sensitization under chronic pain conditions. Blocking NMDA receptors led to an antinociceptive effect in various preclinical chronic pain models and in clinical practice [7, 8]. Genetic knockdown/knockout of spinal cord PSD-95 or PSD-93 attenuated neuropathic pain [9–11]. However, as both NMDA receptors and PSD-95/PSD-93 are expressed widely in the central nervous system and are involved in many physiological processes, directly targeting NMDA receptors or PSD-95/PSD-93 may produce unwanted effects such as cognitive dysfunction, mental disorders, and ataxia [12, 13]. These effects limit the clinical use of the NMDA receptor antagonists and PSD-95/PSD-93 blockers. Hence, targeting downstream signals of NMDA receptors-PSD-95/PSD-93 such as the interaction between nNOS and PSD-95/PSD-93 may serve as a promising strategy in chronic pain management. This strategy may not produce severe side effects, because normal expression and function of NMDA receptors and PSD-95/PSD-93 is maintained [14]. Indeed, systemic administration of ZL006, a small molecular inhibitor of the PSD-95–nNOS interaction, alleviated nociceptive hypersensitivity in various chronic pain models [15–17]. However, repeated and prolonged administration of ZL006 led to significant analgesic tolerance in treatment of neuropathic pain due to GABAergic disinhibition [18, 19]. Recently, the dual-target compound ZL006-05 that blocks the PSD-95–nNOS interaction and selectively potentiates α2-containing $GABA_A$ receptor was developed [19]. Although this new compound has been demonstrated as an antinociception in peripheral nerve trauma–induced neuropathic pain without analgesic tolerance [19], whether it also has similar effects on cancer pain and CIPNP is unknown. Moreover, whether the PSD-95–nNOS interaction participates in the development and maintenance of cancer pain and CIPNP is elusive.

In the present study, we first carried out a mouse model of bone cancer pain induced by inoculating prostate tumor cells (RM-1) into the tibia and examined the effect of systemic administration of ZL006-05 on the development and maintenance of RM-1–induced bone cancer pain. We also conducted a mouse model of CIPNP induced by intraperitoneal injection of paclitaxel and observed the effect of systemic administration of ZL006-05 on the maintenance of paclitaxel-induced neuropathic pain. Finally, we observed whether the ZL006-05's effect was mediated by disrupting the PSD-95–nNOS interaction and enhancing $GABA_A$ receptor function in the pain-related regions.

Materials and Methods

Animal Preparations

Eight-week-old male C57/BL6 mice and CD1 mice (Charles River Lab., Wilmington, MA, USA) were used in the experiments. They were housed in a temperature-controlled room with a standard 12-h light–dark cycle and had free access to food and water. Mice were habituated to the testing environment daily for 3 days before behavioral testing. The experiments were conducted with the approval of the Animal Care and Use Committee at Rutgers New Jersey Medical School and in accordance with the ethical guidelines of the US National Institutes of Health and the International Association for the Study of Pain. All efforts were made to minimize the suffering of animals and reduce the number of animals used. During all behavioral tests, the experimenters were blinded to the treated conditions.

Cell Line and Drugs

Mouse prostate tumor cell line, RM-1, was obtained from American Type Culture Collection (ATCC, Manassas, VA, USA). GABA, isoguvacine, picrotoxin, baclofen, and CGP 55,845 were purchased from Sigma-Aldrich (St. Louis, MO, USA). ZL005, ZL006, and ZL006-05 were kindly provided by Fei Li at Nanjing Medical University School of Pharmacy (Nanjing, China) [15, 19]. Their chemical structures have been reported in previous studies [14, 19, 20]. All of them were dissolved in vehicle 1 (5% $NaHCO_3$ plus 2% Tween 80). Paclitaxel was purchased from Thermo Fisher Scientific and dissolved in vehicle 2 (a mixture of ethanol and Cremophor EL (1:1)). All drugs used in vivo experiments were administered through the tail vein.

Prostate Tumor Cell Preparation

The RM-1 was grown in RPMI 1640 medium (Sigma, St. Louis, MO, USA) that contained L-glutamine and was supplemented with 250 nM dexamethasone and 10% fetal bovine serum. The cells were maintained in T-75 plastic flasks (Corning glass) and cultured in a humidified incubator with 5% CO_2. To collect the cells, they were detached by rinsing gently with calcium- and magnesium-free Hanks' balanced salt solution (HBSS) and a trypsin–EDTA solution. After centrifugation for 3 min at 1200 rpm, the resulting pellet was washed twice with calcium- and magnesium-free HBSS. The final pellet was re-suspended in 1 ml of HBSS. A hemocytometer and trypan blue solution were used to count the cells. The final concentration of 4.5×10^5 cells/15 µl HBSS was used and kept on ice for injection.

Animal Models

RM-1–induced bone cancer pain model was carried out as previously described [21–23]. In brief, the mice were anesthetized with 3% isoflurane and maintained with 1–1.5% isoflurane. After the unilateral leg was shaved, the skin was disinfected with 70% (v/v) ethanol. A 0.5-cm incision was made in the skin over the upper medial half of the tibia. The tibia was carefully exposed with minimal damage to the muscle. The bone was pierced with a 30-gauge needle 5 mm below the knee joint and medial to the medullary canal. Five microliters of RM-1 or HBSS was inoculated into the cavity using a 20-μl Hamilton syringe (with a 27-gauge needle). The syringe was removed 2 min after inoculation. The bone hole was sealed with bone wax (Ethicon, Somerville, NJ, USA), and the skin was sutured with 4–0 silk threads.

Paclitaxel-induced neuropathic pain model was carried out according to the protocol previously described [24, 25]. Briefly, paclitaxel (4 mg/kg; dissolved in the vehicle) or vehicle (a mixture of ethanol and Cremophor EL (1:1)) was injected intraperitoneally every other day for 4 consecutive days (days 1, 3, 5, and 7; 16 mg/kg in total dose).

Behavioral Testing

Mechanical tests were performed as described previously [26, 27]. In brief, each mouse was placed in a Plexiglas chamber on an elevated mesh screen. Two calibrated von Frey filaments (0.07 g and 0.4 g; Stoelting Co., Wood Dale, IL, USA) were applied to the hind paw for approximately 1 s. Each application was repeated 10 times to both hind paws. The occurrence of paw withdrawal in each of these 10 trials was expressed as a percent response frequency ((number of paw withdrawals/10 trials) × 100 = % response frequencies). This percentage was used as an indication of the amount of paw withdrawal.

Thermal tests were carried out following the protocol as reported previously [26, 27]. Briefly, each mouse was placed in a Plexiglas chamber on a glass plate. A radiant heat from Model 336 Analgesic Meter (IITC, Inc./Life Science Instruments, Woodland Hills, CA, USA) was applied to the middle of the plantar surface of each hind paw through the glass plate. When the animal lifted its foot, the light beam was automatically turned off. The length of time between the start of the light beam and the foot lift was defined as the paw withdrawal latency. Each trial was repeated five times at 5-min intervals for each side. A cutoff time of 20 s was used to avoid tissue damage to the hind paw.

Cold tests were performed to the measurement of paw withdrawal latency to noxious cold (0 ℃) as described previously [26, 27]. Briefly, each mouse was placed in a Plexiglas chamber on the cold aluminum plate with continuous temperature monitoring by a thermometer. The length of time between the placement and the sign of mouse jumping was defined as the paw withdrawal latency. Each trial was repeated three times at 10-min intervals. A cutoff time of 20 s was used to avoid tissue damage.

Spontaneous pain behaviors were examined in RM-1–induced bone cancer pain model as described previously [28]. Briefly, mice were placed in the Plexiglas chamber with the wire grid bottom and allowed to acclimate to the chamber for 0.5 h. Guarding and flinching behaviors were measured during the 2-min observation period. Flinching was characterized by rapid flexion and lifting of the ipsilateral hind paw without locomotion. The number of flinches was counted. Guarding was characterized by the retraction of the ipsilateral hind limb under the torso. The time spent guarding the foot (the foot was lifted off of the floor) was measured.

Locomotor functional tests including placing, grasping, and righting reflexes were carried out as described previously [26, 27] before the mice were euthanized. For the placing reflex, the hind limbs were placed slightly lower than the forelimbs and the dorsal surfaces of the hind paws were brought into contact with the edge of a table. Then, whether the hind paws were placed on the table surface reflexively was recorded. For the grasping reflex, the mice were placed on a wire grid, and then whether the hind paws grasped the wire on was recorded. For the righting reflex, the mice were placed on its back on a flat surface. Whether mouse could immediately assume the normal upright position was recorded. Each trial was repeated five times with 5-min intervals, and the score for each test was recorded by counting times of each normal reflex.

Subcellular Fractionation

Subcellular fractionation was carried out as described in previous studies [11, 15]. Briefly, spinal cord tissues were homogenized in the buffer containing 250 mM sucrose, 10 mM Tris–HCl (pH 7.4), 1 mM EDTA, and 1 mM PMSF and 1 mM benzamidine. After homogenization, the homogenate was centrifuged for 15 min at 1,000 × *g* at 4 °C. The supernatant (total soluble fraction) was collected. About 10% of the supernatant was used as input, and the remaining was re-centrifuged at 20,000 × *g* for 20 min at 4 °C. The pellet (crude plasma membrane fraction) was harvested.

Co-immunoprecipitation Assay

Co-immunoprecipitation (Co-IP) assay was carried out based on the previous protocols with minor modifications [11, 15]. In brief, crude plasma membrane fraction harvested above was dissolved in ice-cold lysis buffer containing 50 mM Tris–HCl (pH 7.4), 150 mM NaCl, 1 mM EDTA-Na, 1% NP-40, 0.02% sodium azide, 0.1% SDS,

0.5% sodium deoxycholate, 1% PMSF, and 1% protease inhibitor cocktails. One microgram of mouse anti-PSD-95 (Santa Cruz Biotechnology) or normal mouse serum was incubated to Dynabeads Protein G (Invitrogen) for 3 h at 4 °C on a rotating shaker. The targeted antigen was immunoprecipitated by incubating the protein sample (600 µg) with Dynabeads–antibody complex in a rotating shaker at 4 °C for overnight. On the second day, the mixture of magnetic beads and bound immunocomplexes was washed with the buffer containing 0.05 M HEPES, 0.15 M NaCl, and 0.15 M Triton-100 (pH 7.4). The bound immunocomplexes were eluted from magnetic beads by heating at 99 °C in 1 × sample loading buffer and analyzed through Western blotting assay as described below.

Western Blotting Assay

Western blotting assay was carried out as described previously described [29–31]. In brief, after mice were euthanized with isoflurane, L3/L4 spinal cord was collected and rapidly frozen in liquid nitrogen. The tissues were homogenized in chilled lysis buffer (10 mM Tris, 5 mM $MgCl_2$, 5 mM EGTA, 250 mM sucrose, 1 mM phenylmethylsulfonyl fluoride, 1 mM DTT, and 40 µM leupeptin). After the homogenates were centrifuged at 4 ℃ for 15 min at 1,000 g, the supernatant was collected. After protein concentration was measured, the samples were heated at 99 ℃ for 5 min and loaded onto a 4–20% precast polyacrylamide gel (Bio-Rad Laboratories). The proteins were then electrophoretically transferred onto 0.2 µm pore-sized nitrocellulose membranes (Bio-Rad Laboratories). The membranes were blocked with 3% non-fat milk in Tris-buffered saline containing 0.1% Tween 20 for 1 h and then incubated with primary antibodies, including rabbit anti-phosphorylated extracellular signal–regulated kinase (phosphorylation of extracellular signal–regulated kinase 1 and 2 (p-ERK1/2), 1:1,000, Cell Signaling), rabbit anti-extracellular signal–regulated kinase (ERK1/2, 1:1,000, Cell Signaling), mouse anti-glial fibrillary acidic protein (glial fibrillary acidic protein (GFAP); 1:1,000, Cell Signaling), rabbit anti-PSD95 (1:1,000, Cell Signaling Technology), rabbit anti-nNOS (1:250, Cell Signaling Technology), and rabbit anti-GAPDH (1:1,000; Santa Cruz Biotechnology, Dallas, TX, USA) at 4 ℃ overnight under gentle agitation. The proteins were detected by goat peroxidase–conjugated anti-mouse antibody (1:3,000, Jackson ImmunoResearch) or anti-rabbit secondary antibody (1:3,000, Jackson ImmunoResearch), developed by Western peroxide reagent and luminol/enhancer reagent (Clarity Western ECL Substrate, Bio-Rad) and visualized using the ChemiDoc XRS System with Image Lab software (Bio-Rad). The intensity of blots was quantified with densitometry using Image Lab software (Bio-Rad).

Electrophysiological Recording

Spinal cord and brain slices were prepared as previously described [11, 30, 31]. CD1 mice (6-week-old) were deeply anesthetized with isoflurane as described above and then perfused through the left ventricle for 2 min with ice-cold sucrose-substituted artificial cerebrospinal fluid (ACSF in mM: 75 sucrose, 80 NaCl, 2.5 KCl, 0.5 $CaCl_2$, 1.2 $MgCl_2$, 1.25 NaH_2PO_4, 25 $NaHCO_3$, 1.3 ascorbate, and 3.0 pyruvate). The lumbosacral spinal cord or brain was quickly removed and placed in ice-cold sucrose ACSF. The fourth (L_4) or fifth (L_5) lumbar spinal cord or brain (which contained the anterior cingulate cortex (ACC)) was sectioned using a vibrating microtome (400–600 µm thickness for spinal cord and 450 µm for brain). The slices were then maintained at room temperature (22–25 °C) in regular ACSF (in mM: 117 NaCl, 3.6 KCl, 2.5 $CaCl_2$, 1.2 $MgCl_2$, 1.2 NaH_2PO_4, 25 $NaHCO_3$, and 11 glucose) equilibrated with 95% O_2 and 5% CO_2. The drugs used in perfusion buffer include 200 µM GABA, 10 µM isoguvacine, 10 µM picrotoxin, 10 µM baclofen, 1 µM CGP 55,845, or different concentrations of ZL006-05.

The whole-cell patch-clamp recordings were made from ACC neurons or lamina II neurons of spinal cord in voltage-clamp mode. Under a dissecting microscope, the substantia gelatinosa (lamina II) was clearly visible as a relatively translucent band across the dorsal horn. Patch pipettes were fabricated from thin-walled, borosilicate, glass-capillary tubing (1.5 mm outer diameter; World Precision Instruments, Sarasota, FL, USA). After establishing the whole-cell configuration, potentials of neurons were held at 0 mV for GABA-induced current. The resistance of a typical patch pipette was 5–8 MΩ when filled with the internal solution (in mM: 110 Cs_2SO_4, 0.5 $CaCl_2$, 2 $MgCl_2$, 5 EGTA, 5 HEPES, 5 tetraethylammonium, and 5 ATP-Mg). Membrane currents were amplified with an Axopatch 700B amplifier (Molecular Devices, Sunnyvale, CA, USA) in voltage-clamp mode. Signals were filtered at 1 kHz and digitized using a Digidata 1550 with pClamp 10.4 software (Molecular Devices). Series resistance was compensated by 60–80%. Cell membrane capacitances were acquired by reading the value for whole-cell capacitance compensation directly from the amplifier. An online P/4 leak subtraction was performed to eliminate leak current contribution. The data were stored on computer by a Digidata 1550 interface and were analyzed by the pClamp 10.4 software package (Molecular Devices).

Statistical Analysis

The mice were assigned into various treatment groups randomly. All results were expressed as mean ± SEM. All of the data were statistically analyzed using two-tailed, paired

Student's *t* test and a one-way or two-way ANOVA. When ANOVAs showed significant differences, pairwise comparisons between the means were analyzed by the post hoc Tukey method (Sigma Plot 12.5, San Jose, CA, USA). Significance was set at $P < 0.05$.

Results

Effects of Systemic ZL006-05 Administration on the Development of RM-1–Induced Bone Cancer Pain

To examine the effect of systemic administration of the dual-target compound ZL006-05 on the development of RM-1–induced bone cancer pain, we intravenously injected vehicle 1 or ZL006-05 at 4 mg/kg once a day for 7 consecutive days after inoculation of HBSS or RM-1 into the tibia. To evaluate whether it has the better effect, we also intravenously injected ZL005 (a small molecular agonist of $GABA_A$ receptor) or ZL006 (a small molecular inhibitor of the PSD-95–nNOS interaction) at the same dosage once a day for 7 consecutive days after inoculation of HBSS or RM-1 into the tibia. Consistent with previous studies [21–23], tibial inoculation of RM-1, but not HBSS, produced robust and long-lasting mechanical allodynia, as demonstrated by significant increases in paw withdrawal frequencies in response to 0.07 g and 0.4 g von Frey filaments, and heat and cold hyperalgesia, as evidenced by marked decreases in paw withdrawal latencies to heat and cold stimuli, respectively, on the ipsilateral side compared with pre-inoculation baseline values in the vehicle 1–treated mice (Fig. 1A–D). These nociceptive hypersensitivities became apparent between days 3 and 5 post-RM-1 inoculation and remained pronounced at least on day 7 post-RM-1 inoculation (Fig. 1A–D). As expected, no significant changes in paw withdrawal frequency or latency were observed on the contralateral side after RM-1 inoculation and on either side after HBSS injection in the vehicle 1–treated mice (Fig. 1A–G). Intravenous (i.v.) administration of ZL006-05 abolished the RM-1–induced mechanical allodynia and heat and cold hyperalgesia on days 3, 5, and 7 post-RM-1 inoculation on

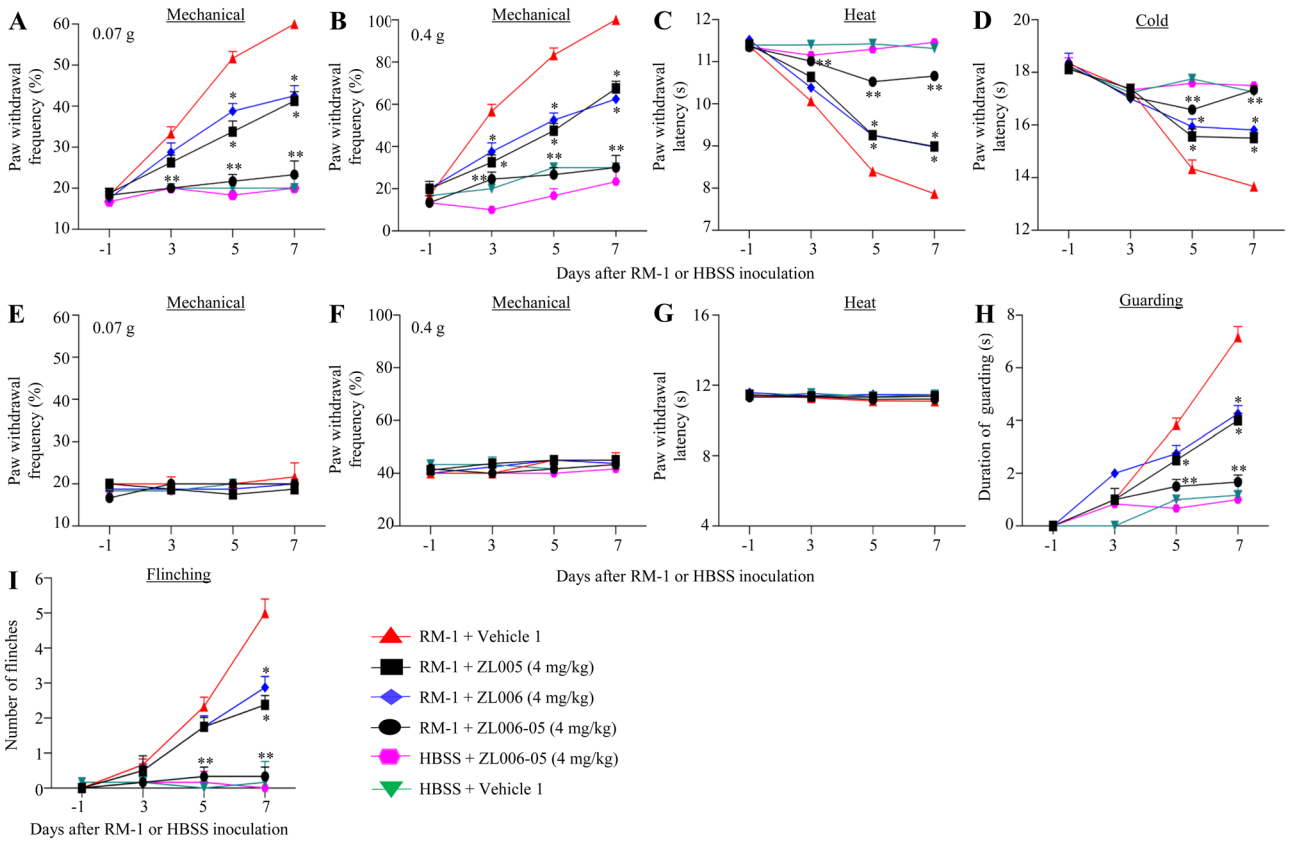

Fig. 1 Effects of systemic pre-administration of ZL006-05, ZL005, and ZL006 on RM-1–induced metastatic bone cancer pain. ZL006-05, ZL005, ZL006, or vehicle 1 was injected via tail vein 30 min before RM-1 or HBSS inoculation and then once daily for 6 consecutive days. Behavioral tests were carried out 1 day before RM-1 or HBSS inoculation and on days 3, 5, and 7 after RM-1 or HBSS inoculation on the ipsilateral (**A**–**D**, **H**, **I**) and contralateral (**E**–**G**) sides. $n = 8$ mice per group. Two-way ANOVA with repeated measures followed by post hoc Tukey test. $^*P < 0.05$, $^{**}P < 0.01$, versus the RM-1 plus vehicle 1 group at the corresponding time point

Table 1 Locomotor function

Treatment group	Placing	Grasping	Righting
HBSS + vehicle 1	5 (0)	5 (0)	5 (0)
HBSS + ZL006-05 (4 mg/kg)	5 (0)	5 (0)	5 (0)
RM-1 + vehicle 1	5 (0)	5 (0)	5 (0)
RM-1 + ZL006-05 (4 mg/kg)	5 (0)	5 (0)	5 (0)
RM-1 + ZL005 (4 mg/kg)	5 (0)	5 (0)	5 (0)
RM-1 + ZL006 (4 mg/kg)	5 (0)	5 (0)	5 (0)
Vehicle 2 + saline	5 (0)	5 (0)	5 (0)
PTX + saline	5 (0)	5 (0)	5 (0)
PTX + ZL006-05 (10 mg/kg)	5 (0)	5 (0)	5 (0)
Vehicle 2 + ZL006-05 (10 mg/kg)	5 (0)	5 (0)	5 (0)

the ipsilateral side (Fig. 1A–D). In contrast, i.v. administration of ZL005 or ZL006 at the same dosage partially attenuated the RM-1–induced mechanical allodynia and heat and cold hyperalgesia on days 3, 5, and 7 post-RM-1 inoculation on the ipsilateral side (Fig. 1A–D). None of these drugs significantly altered basal paw withdrawal responses on the contralateral side in the RM-1–treated mice (Fig. 1E–G). In addition, intravenous ZL006-05 administration did not affect basal paw withdrawal responses on both sides in the HBSS-treated mice (Fig. 1A–G).

The vehicle 1–treated mice with tibial inoculation of RM-1 also displayed spontaneous pain as evidenced by significant increases in the duration of guarding behavior and the number of flinches on days 5 and 7 post-RM-1 inoculation (Fig. 1H, I). These spontaneous pain behaviors were abolished by i.v. administration of ZL006-05 and partially blocked by i.v. administration of ZL005 or ZL006 (Fig. 1H, I). All treated mice displayed normal locomotor activity as demonstrated by no marked differences in placing, grasping, and righting reflexes among these mice (Table 1).

We also examined whether i.v. administration of ZL006-05 affected the RM-1–induced dorsal horn neuronal/glial hyperactivities as demonstrated by increases in p-ERK1/2 (a marker for neuronal hyperactivation) and GFAP (a marker for astrocyte hyperactivation) in dorsal horn during the development period. Levels of p-ERK1/2 and GFAP significantly increased in the ipsilateral L3/L4 dorsal horn on day 7 after RM-1 inoculation in the vehicle 1–treated mice compared with the HSBB-inoculated mice treated with vehicle 1 (Fig. 2). These increases were absent in the ZL006-05–treated RM-1 mice (Fig. 2). Intravenous administration of ZL006-05 did not alter basal expression of p-ERK1/2, total ERK1/2, or GFAP in the dorsal horn of the HSBB-inoculated mice (Fig. 2).

Effects of Systemic ZL006-05 Administration on the Maintenance of RM-1–Induced Bone Cancer Pain

To further examine whether systemic administration of ZL006-05 on the maintenance of RM-1–induced bone cancer pain, we intravenously injected vehicle 1 or ZL006-05 at different doses once a day for 8 consecutive days starting at day 7 post-RM-1 inoculation. Intravenous administration of ZL006-05 produced a dose-dependent effect on RM-1–induced mechanical allodynia, heat and cold hyperalgesia, and spontaneous pain on days 10, 12, and 14 post-RM-1 inoculation on the ipsilateral side (Fig. 3A–D, H, I). On day 14 after RM-1 inoculation, i.v. ZL006-05 reduced paw withdrawal frequencies in response to 0.07 g and 0.4 g von Frey filaments by 62% and 50%, respectively, at the dose of 4 mg/kg and by 38% and 26%, respectively, at the dose of 2 mg/kg compared with the corresponding RM-1–inoculated group treated with vehicle 1 (Fig. 3A, B). The 0.4 mg/kg of i.v. ZL006-05 had no effect on the RM-1–induced increases in paw withdrawal frequencies

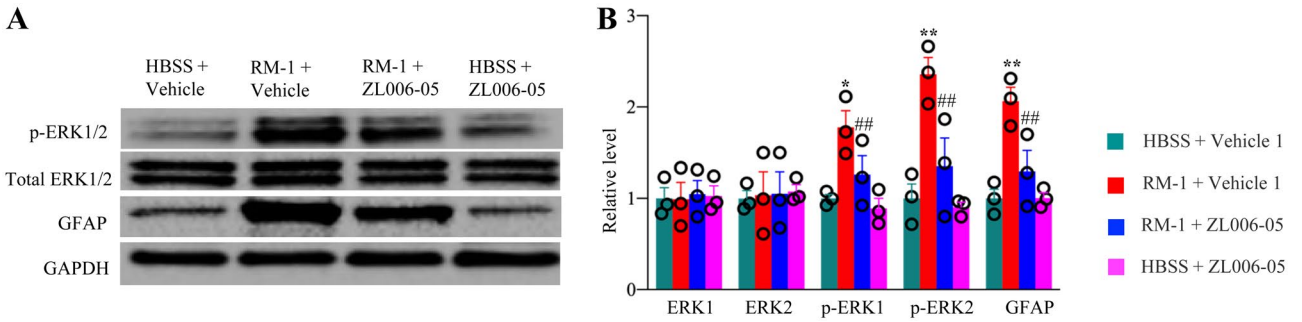

Fig. 2 Effect of systemic pre-administration of ZL006-05 (4 mg/kg) on the RM-1–induced neuronal and glial hyperactivities in dorsal horn. The levels of the phosphorylation of ERK1/2 (p-ERK1/2), total ERK1/2, and GFAP in the ipsilateral lumbar 3/4 dorsal horn on day 7 post-RM-1 or vehicle 1 inoculation. Representative Western blots (**A**) and a summary of densitometric analysis (**B**) are shown. $n=3$ biological repeats (3 mice) per group. One-way ANOVA followed by post hoc Tukey test, $^{*}P<0.05$, $^{**}P<0.01$, versus the corresponding HBSS plus vehicle 1 group. $^{\#\#}P<0.01$, versus the corresponding RM-1 plus vehicle 1 group

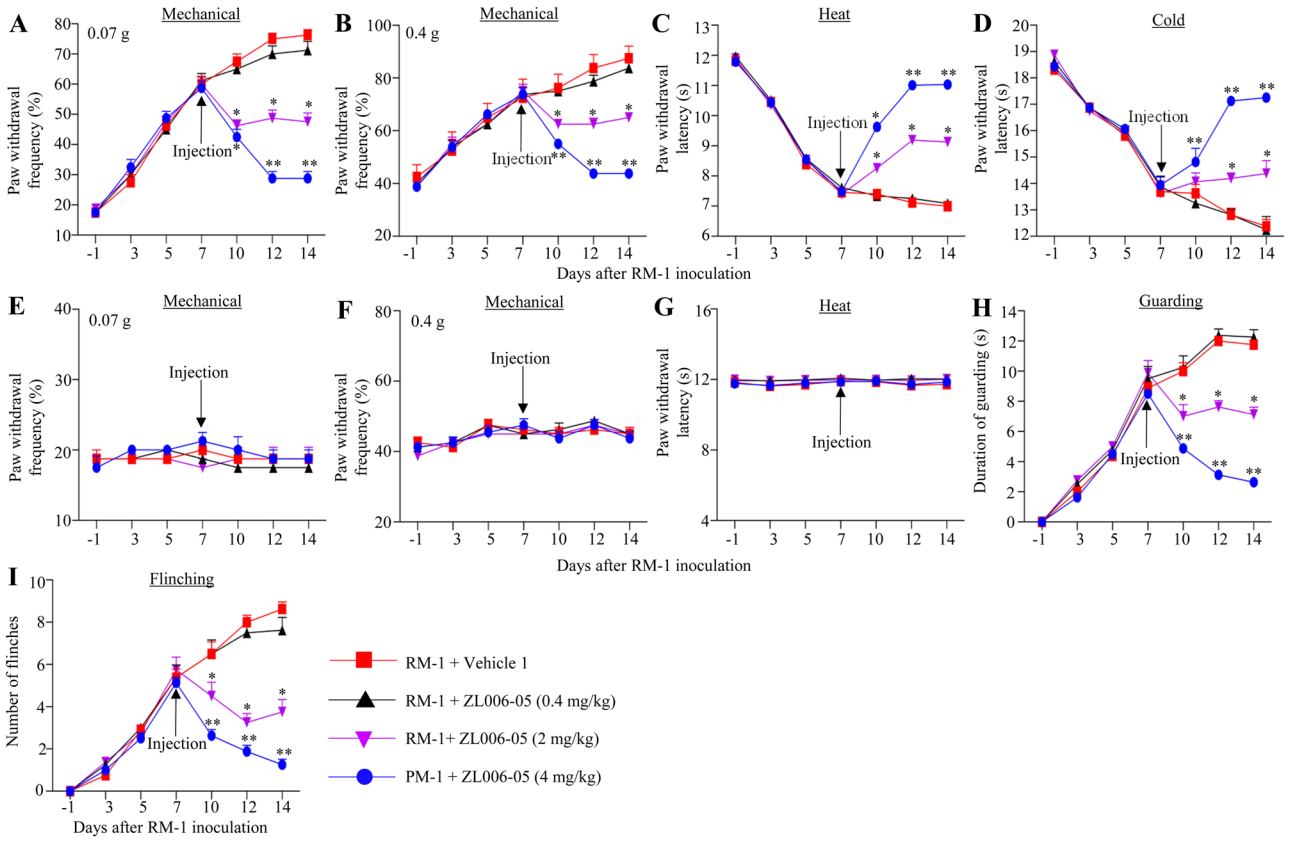

Fig. 3 Effects of systemic post-administration of ZL006-05 at different dosages (0.4 mg/kg, 2 mg/kg, and 4 mg/kg) on RM-1–induced metastatic bone pain. ZL006-05 or vehicle 1 was injected via tail vein once daily for 8 consecutive days starting on day 7 after RM-1 inoculation. Behavioral tests were carried out 1 day before RM-1 or HBSS inoculation and on days 3, 5, 7, 10, 12, and 14 after RM-1 or HBSS inoculation on the ipsilateral (**A**, **D**, **H**, **I**) and contralateral (**E**–**G**) sides. $n = 8$ mice per group. Two-way ANOVA with repeated measures followed by post hoc Tukey test. $^{*}P < 0.05$, $^{**}P < 0.01$, versus the RM-1 plus vehicle 1 group at the corresponding time point

(Fig. 3A, B). Similarly, on day 14 post-RM-1 inoculation, i.v. ZL006-05 increased paw withdrawal latencies in response to heat and cold stimuli by 1.58-fold and 1.39-fold, respectively, at the dose of 4 mg/kg and by 1.21-fold and 1.16-fold, respectively, at the dose of 2 mg/kg, but had no effect at the dose of 0.4 mg/kg compared with the corresponding RM-1–inoculated group treated with vehicle 1 (Fig. 3C, D). The duration of guarding and the number of flinches were reduced through i.v. ZL006-05 by 78% and 86%, respectively, at the dose of 4 mg/kg, by 39% and 57%, respectively, at the dose of 2 mg/kg and by − 4% and 12%, respectively, at the dose of 0.4 mg/kg in the RMM-1–inoculated mice compared with the corresponding RM-1–inoculated mice treated with vehicle 1 on day 14 post-RM-1 inoculation (Fig. 3H, I). As expected, none of three doses of ZL006-05 alters basal paw withdrawal responses to mechanical, heat and cold stimuli applied to the contralateral hind paw during the maintenance period (Fig. 3E–G).

Effects of Systemic ZL006-05 Administration on the Maintenance of Paclitaxel-Induced Neuropathic Pain

Consistent with the previous reports [24, 25], intraperitoneal (i.p.) injection of paclitaxel, but not vehicle 2, produced dramatic and long-lasting mechanical allodynia, heat hyperalgesia, and cold hyperalgesia on both sides in the vehicle 1–treated mice (Fig. 4A–G). These nociceptive hypersensitivities occurred on day 7 after the first i.p. paclitaxel injection and persisted for at least 15 days (Fig. 4A–G). To investigate the effect of systemic administration of ZL006-05 on the maintenance of paclitaxel-induced nociceptive hypersensitivity, we intravenously administered ZL006-05 or vehicle 1 once a day for 7 consecutive days starting on day 9 after the first i.p. injection of paclitaxel or vehicle 2. Intravenous administration of ZL006-05 at 10 mg/kg significantly reduced the paclitaxel-induced increases in paw withdrawal frequencies

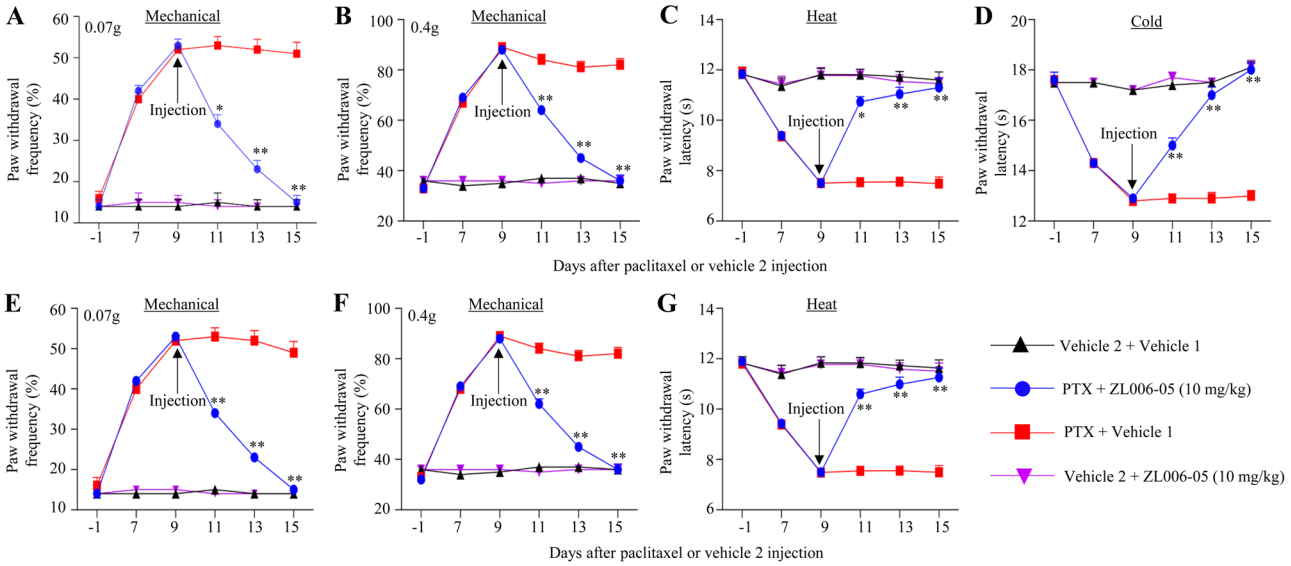

Fig. 4 Effects of systemic post-administration of ZL006-05 on paclitaxel-induced neuropathic pain. ZL006-05 (10 mg/kg) or vehicle 1 was injected via tail vein once daily for 7 consecutive days starting on day 9 after intraperitoneal paclitaxel or vehicle 2 injection. Behavioral tests were carried out 1 day before paclitaxel or vehicle 2 injection and on days 7, 9, 11, 13, and 15 after paclitaxel or vehicle 2 injection on the ipsilateral (**A**–**D**) and contralateral (**E**–**G**) sides. $n = 10$ mice per group. Two-way ANOVA with repeated measures followed by post hoc Tukey test. $^{*}P < 0.05$, $^{**}P < 0.01$, versus the paclitaxel plus vehicle 1 group at the corresponding time point

in responses to 0.07 g and 0.4 g von Frey filaments and blocked the paclitaxel-induced decreases in paw withdrawal latencies in responses to heat and cold stimuli on days 11, 13, and 15 after the first i.p. injection of paclitaxel on both ipsilateral and contralateral sides (Fig. 4A–G). These effects of ZL006-05 were dose-dependent (Fig. 5A–G). As expected, i.v. ZL006-05 at 10 mg/kg did not alter basal paw withdrawal responses to mechanical, heat, and cold stimuli

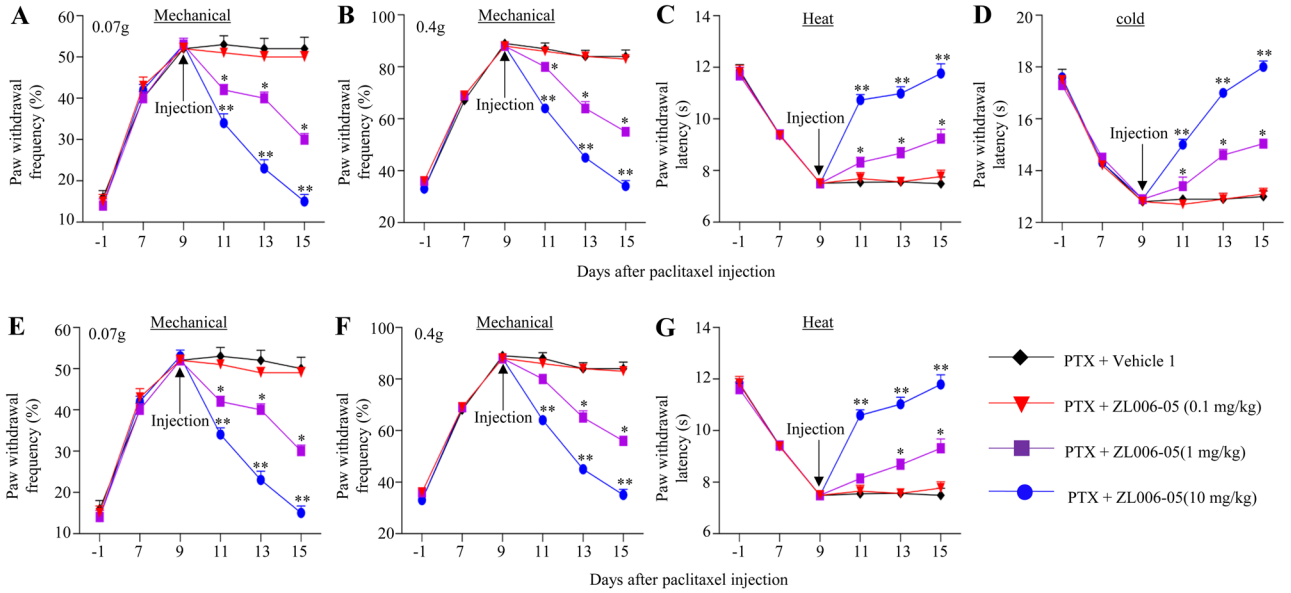

Fig. 5 Effects of systemic post-administration of ZL006-05 at different dosages (0.1 mg/kg, 1 mg/kg, and 10 mg/kg) on paclitaxel-induced neuropathic pain. ZL006-05 or vehicle 1 was injected via tail vein once daily for 7 consecutive days starting on day 9 after intraperitoneal paclitaxel injection. Behavioral tests were carried out 1 day before paclitaxel injection and on days 7, 9, 11, 13, and 15 after paclitaxel injection on the ipsilateral (**A**–**D**) and contralateral (**E**–**G**) sides. $n = 10$ mice per group. Two-way ANOVA with repeated measures followed by post hoc Tukey test. $^{*}P < 0.05$, $^{**}P < 0.01$ versus the paclitaxel plus vehicle 1 group at the corresponding time point

on both sides in the vehicle 2–treated mice (Fig. 4A–G). All treated mice displayed normal locomotor activity (Table 1).

We further investigated whether i.v. administration of ZL006-05 affected the paclitaxel-induced dorsal horn neuronal/glial hyperactivities. Like in the RM-1–induced bone cancer pain model described above, levels of p-ERK1/2 and GFAP markedly increased in the bilateral L3/L4 dorsal horn on day 15 after the first i.p. injection of paclitaxel in the vehicle 1–treated mice compared with the vehicle 2–injected mice treated with vehicle 1 (Fig. 6). These increases were not seen in the ZL006-05–treated paclitaxel mice (Fig. 6). Intravenous administration of ZL006-05 did not affect the basal expression of p-ERK1/2, total ERK1/2, or GFAP in the dorsal horn of the vehicle 2–injected mice (Fig. 6).

ZL006-05 Potentiates the GABA-Evoked Currents Through $GABA_A$ Receptor in the Neurons of Dorsal Horn and Anterior Cingulate Cortex

The previous study has demonstrated the potentiation of GABA-evoked currents by ZL006-05 through α2-containing $GABA_A$ receptor in the HEK-293 cells [19]. To further verify ZL006-05 function in the neurons from the pain-associated regions in the central nervous system, we recorded the GABA-evoked currents in lamina II neurons of dorsal horn by holding the voltage at 0 mV under the perfusion with ZL006-05 at the different concentrations (0 μM (control), 0.1 μM, 1 μM, 10 μM, and 100 μM). Approximately 61% of the neurons (11 of 18) recorded with GABA-evoked currents responded to ZL006-05. Compared to the control group, the amplitudes of GABA-evoked currents were increased by 1.42-fold at 1 μM ZL006-05, by 1.71-fold at 10 μM ZL006-05, and by 1.68-fold at 100 μM ZL006-05 (Fig. 7A, B). Furthermore, the amplitude of the current evoked by the $GABA_A$ selective agonist isoguvacine (10 μM) was also significantly increased by 1.57-fold at 10 μM ZL006-05 compared to the control group (Fig. 7C, D). This increased current could be completely blocked through co-perfusion with the $GABA_A$-selective antagonist picrotoxin (10 μM; Fig. 7C), suggesting that $GABA_A$ receptor mediates the ZL006-05's potentiated action on GABA-evoked current. To substantiate this action, we assessed the effect of ZL006-05 on $GABA_A$ agonist's concentration-dependent response curve in lamina II neurons by examining the effect of 10 μM ZL006-05 on the currents induced by different concentrations of isoguvacine. ZL006-05 produced a significant left shift in the concentration–response curves to isoguvacine (Fig. 7E). The EC50 values in the absence and presence of ZL006-05 were 38.22 ± 3.3 μM and 5.12 ± 3.1 μM, respectively (Fig. 7E). In addition, we observed that the amplitude of isoguvacine-evoked current was markedly increased by 1.53-fold at 10 μM ZL006-05 in the neurons of anterior cingulate cortex (Fig. 7F, G). In contrast, ZL006-05 at 10 μM had no effect on baclofen (a $GABA_B$-selective agonist, 10 μM)-induced current, although this evoked current could be completely blocked by CGP 55,845, a $GABA_B$-selective antagonist (Fig. 7H, I).

Systemic ZL006-05 Administration Disrupts the PSD-95–nNOS Interaction in Dorsal Horn

Besides the $GABA_A$ receptor potentiation, we finally examined whether systemic ZL006-05 administration also affected the PSD-95–nNOS interaction in the dorsal horn. In the crude plasma membrane fraction from spinal dorsal horn, the level of nNOS and the binding density of PSD-95–nNOS in the paclitaxel plus vehicle 1–treated group were markedly increased by 1.51-fold and 1.88-fold, respectively, compared to those in the vehicle 2 plus vehicle 1–treated group (Fig. 8A–C). These increases were attenuated in the ZL006-05 plus paclitaxel–treated group (Fig. 8A–C). The basal level of PSD-95 in the crude plasma membrane (Fig. 8A, B) and total amounts of nNOS and PSD-95 in whole membrane and cytoplasmic lysis (Fig. 8D, E)

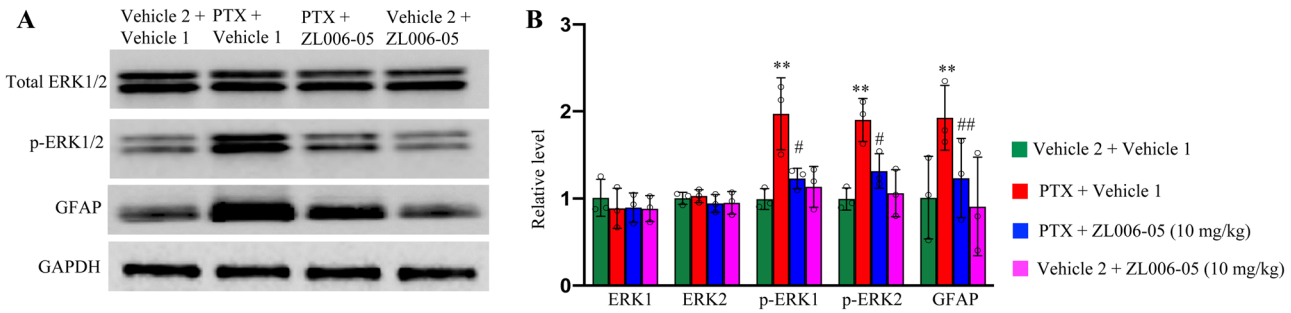

Fig. 6 Effect of systemic post-administration of ZL006-05 (10 mg/kg) on the paclitaxel-induced neuronal and glial hyperactivities in dorsal horn. The levels of the phosphorylation of ERK1/2 (p-ERK1/2), total ERK1/2, and GFAP in the lumbar enlargement dorsal horn on day 15 post-paclitaxel or vehicle 2 injection. Representative Western blots (**A**) and a summary of densitometric analysis (**B**) are shown. $n = 3$ biological repeats (3 mice) per group. One-way ANOVA followed by post hoc Tukey test, $^{**}P < 0.01$, versus the corresponding vehicle 1 plus vehicle 2 group. $^{\#}P < 0.05$, $^{\#\#}P < 0.01$, versus the corresponding paclitaxel plus vehicle 1 group

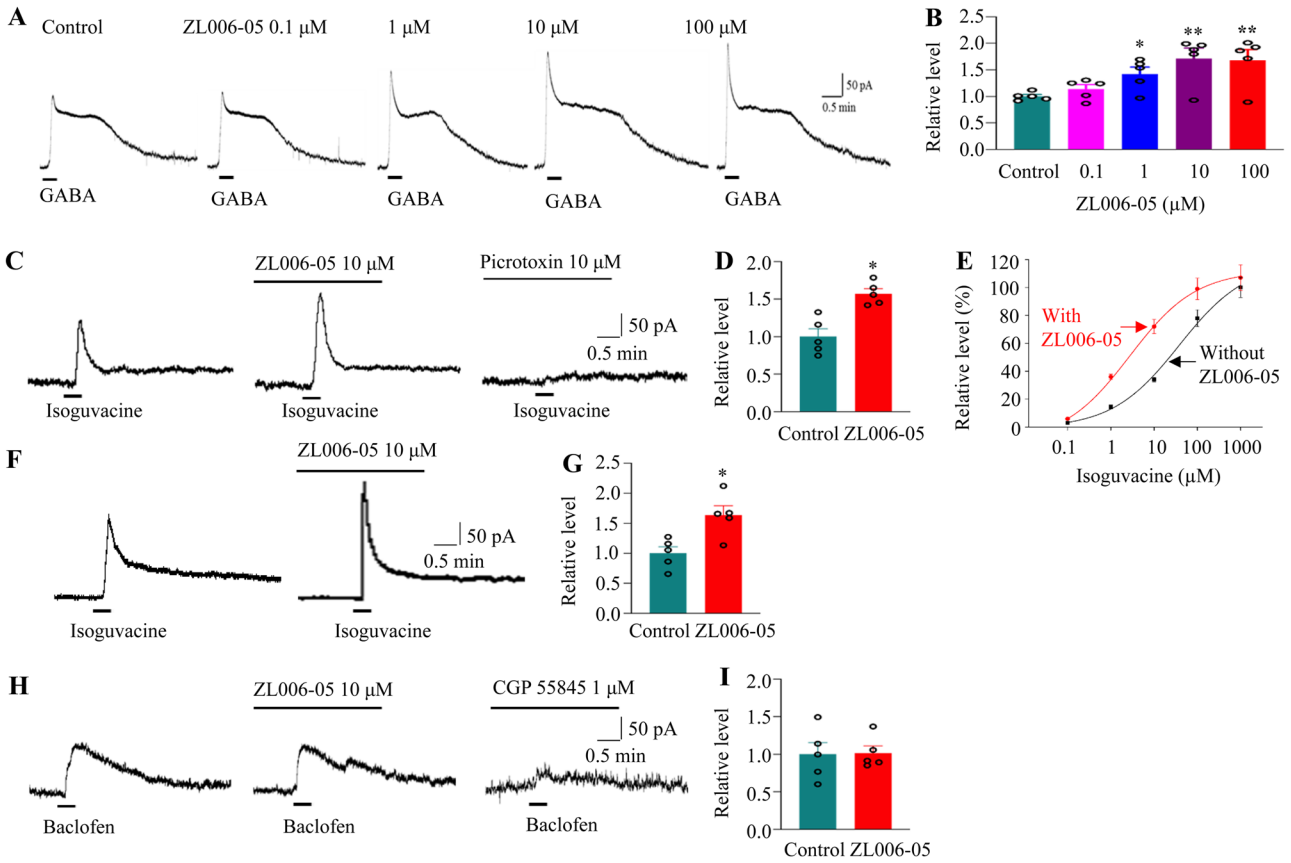

Fig. 7 ZL006-05 potentiates the GABA-evoked currents through the $GABA_A$ receptor in the neurons of spinal dorsal horn and anterior cingulate cortex. **A**, **B** Effects of different concentrations of ZL005-06 (0 μM (control), 1 μM, 10 μM, and 100 μM) on GABA (200 μM)-induced currents recorded at a holding potential of 0 mV in lamina II neurons of dorsal horn. Representative current traces from one neuron (**A**) and quantification of GABA-induced currents in typical consecutive recording neurons from 18 mice (**B**). The response values were normalized to the control group. $n=5$ neurons per concentration. One-way ANOVA followed by post hoc Tukey test. $^*P<0.05$, $^{**}P<0.01$, versus the control group. **C**, **D** Effects of ZL005-06 or picrotoxin on isoguvacine (10 μM)-evoked currents recorded at a holding potential of 0 mV in lamina II neurons of dorsal horn. Representative current traces from one neuron (**C**) and quantification of isoguvacine-evoked currents in the absence or presence of ZL005-06 (**D**). $n=5$ neurons (from 5 mice) per group. $^*P<0.05$, versus the control group by two-tailed paired Student's *t* test. **E** The graph showed the concentration (*x*-axis)–response (*y*-axis) relationship of isoguvacine in the absence or presence of ZL005-06. The response values were normalized to one at 1,000 μM isoguvacine in each neuron. $n=5$ neurons (from 5 mice) per concentration. **F**, **G** Effects of ZL005-06 (10 μM) on isoguvacine (10 μM)-evoked currents in the neurons of anterior cingulate cortex. Representative current traces from one neuron (**F**) and quantification of isoguvacine-evoked currents in the absence or presence of ZL005-06 (**G**). $n=5$ neurons (from 5 mice) per group. $^*P<0.05$, versus the control group by two-tailed paired Student's *t* test. **H**, **I** Effects of ZL005-06 or CGP 55845 on baclofen (10 μM)-evoked currents in lamina II neurons of spinal dorsal horn. Representative current traces from one neuron (**H**) and quantification of baclofen-evoked currents in the absence or presence of ZL005-06 (**I**). $n=5$ neurons (from 5 mice) per group

from the spinal dorsal horn of the paclitaxel plus vehicle 1– or ZL006-06–treated group were not significantly altered compared with the vehicle 2 plus vehicle 1–treated group (Fig. 7A, B, D, E).

Discussion

The inoculation of RM-1 into tibia and i.p. injection of paclitaxel leads to robust and long-lasting evoked nociceptive hypersensitivity and ongoing spontaneous pain in mice, which mimics clinical symptoms of many patients with bone metastases and chemotherapy, respectively. Understanding the mechanisms underlying RM-1–induced cancer bone pain and paclitaxel-induced neuropathic pain may provide novel strategies for the management of these two disorders. Although intensive research into metastatic bone pain and CIPNP has been carried out in the past decades, effective treatment without unwanted side effects for these two disorders is still lacking. The present study showed that systemic administration of ZL006-05 dose-dependently attenuated RM-1–induced bone cancer pain

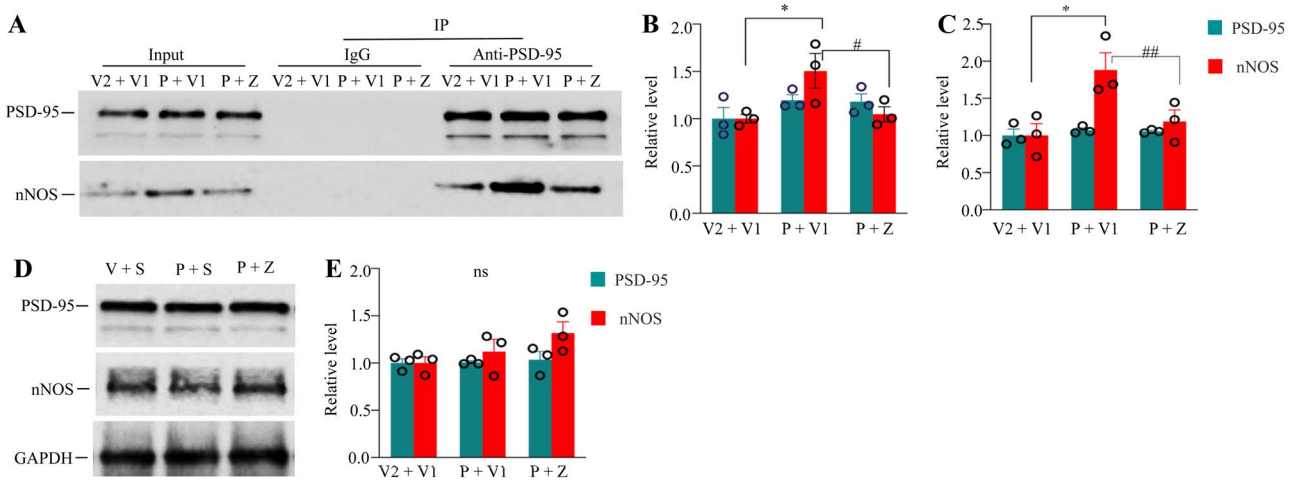

Fig. 8 Effect of systemic post-administration of ZL006 on the paclitaxel-induced increase in the PSD-95–nNOS interaction in the lumbar dorsal horn 15 days after intraperitoneal paclitaxel or vehicle 2 injection. V1: vehicle 1. V2: vehicle 2. P: paclitaxel. Z: ZL006-005. **A**–**C** Levels of PSD-95 and nNOS in the crude membrane fraction before (Input) and after co-immunoprecipitation (IP) with anti-PSD-95 serum or normal serum (IgG) from the lumbar dorsal horn of the mice treated as indicated. The band densities for the vehicle 1 plus vehicle 2–treated groups were set as 100%. The relative densities from the remaining groups were determined by dividing the optical densities from these groups by the values of the corresponding vehicle 1 plus vehicle 2–treated groups. **A** Representative Western blots. **B** A summary of densitometric analysis from Input. **C** A summary of densitometric analysis after Co-IP. $n = 3$ biological repeats (6 mice) per group. One-way ANOVA followed by post hoc Tukey test. $^{*}P < 0.05$, versus the corresponding vehicle 1 plus vehicle 2–treated group. $^{\#}P < 0.05$, $^{\#\#}P < 0.01$, versus the corresponding paclitaxel plus vehicle 1–treated group. **D** Total levels of nNOS and PSD-95 in the cytosolic and membrane fractions from the lumbar spinal dorsal horn of the different treated groups indicated. $n = 3$ biological repeats (3 mice) per group. GAPDH was used as a loading control

and paclitaxel-induced neuropathic pain. Mechanistically, ZL006-05 not only disrupted the PSD-95–nNOS interaction but also potentiated the $GABA_A$ receptor function in dorsal horn neurons. These findings suggest that the $GABA_A$ receptor as well as the protein–protein interaction between PSD-95 and nNOS in the dorsal horn are required for the genesis of metastatic bone cancer pain and CIPNP. ZL006-05 may be a potential drug for the management of these two disorders.

The PSD-95–nNOS interaction contributes to the development and maintenance of chronic pain. PSD-95 binds to nNOS in the neurons of dorsal horn and thalamus [10, 15]. Systemic administration of small compounds such as ZL006 that disrupted this binding suppressed the formalin-induced second nociceptive behaviors, complete Freund's adjuvant–induced inflammatory pain, chronic constriction injury/spinal nerve injury–induced neuropathic pain, and hemorrhage-induced thalamic pain [15–17, 19, 32]. The present study further demonstrated that systemic injection of ZL006-05 attenuated the RM-1–induced metastatic bone cancer pain and paclitaxel-induced neuropathic pain. Systemic injection of ZL006-05 also suppressed RM-1–induced or paclitaxel-induced hyperactivities of dorsal horn neurons and astrocytes, evidenced by blockage of the RM-1–induced or paclitaxel-induced increases in dorsal horn p-ERK1/2 and GFAP, respectively. Thus, the anti-nociceptive effects caused by systemic ZL006-05 likely result from the attenuation of central sensitization due to suppression in neuronal and glia hyperactivities in dorsal horn under the conditions of cancer pain and chemotherapy-induced neuropathic pain. Taken together, the data from previous studies and the present work indicate that the PSD-95–nNOS interaction participates in nociceptive hypersensitivity in various chronic pain models.

Compared to other small single-target compounds (e.g., ZL006), ZL006-05 is a dual-target compound that was made by linking ZL006 and (+)-borneol through an ester bond [19]. Indeed, the previous study showed that ZL006-05 disturbed the PSD-95–nNOS binding in dorsal horn, potentiated GABA-evoked currents in the HEK293 cells expressing α2-containing $GABA_A$ receptor, and increased the amplitude in miniature inhibitory postsynaptic currents (but not miniature excitatory postsynaptic currents) in lamina I neurons of dorsal horn [19]. The present study further demonstrated that this compound not only disrupted the PSD-95–nNOS interaction in spinal dorsal horn, but also potentiated the amplitude of $GABA_A$ receptor in the neurons of dorsal horn lamina II and anterior cingulate cortex. Moreover, we found that ZL006-05 had the stronger antinociceptive effect on RM-1–induced bone cancer pain compared with ZL006 and ZL005 at the same dosage. It appears that this stronger effect is likely attributed to the

blockade of NMDA receptor/PSD-95/nNOS signaling pathway and potentiation of $GABA_A$ receptor–mediated inhibitory pathway in dorsal horn and anterior cingulate cortex. However, given that PSD-95/nNOS and $GABA_A$ receptor are widely expressed in the neurons of the central nervous system, the effect of systemic administration of ZL006-05 on bone cancer pain and CIPNP by dually targeting these two pathways in the neurons from other pain-associated brain regions could be ruled out.

Besides being highly effective against chronic pain, systemic administration of ZL006-05 did not show unwanted side effects. Unlike ZL006, chronic intrathecal application of ZL006-05 did not produce analgesic tolerance and maintained its antinociceptive effect during a 28-day treatment of spinal nerve injury–induced neuropathic pain [19]. Consistently, the present study also demonstrated that repeated i.v. administrations of ZL006-05 for 7 to 8 consecutive days led to the time-dependent antinociceptive effect on both bone cancer pain and paclitaxel-induced neuropathic pain without analgesic tolerance. In addition, systemic administration of ZL006-05 did not alter basal (acute) pain and locomotor activity and had no effect on spatial memory observed in the present study and previous work [19]. Taken together, the evidence strongly suggests that ZN006-05 may have the potential application in the management of chronic pain including cancer pain and CIPNP.

Supplementary Information The online version contains supplementary material available at https://doi.org/10.1007/s13311-021-01158-8.

Acknowledgements The authors thanked Dr. Fei Li from Nanjing Medical University School of Pharmacy for generously providing ZL005, ZL006, and ZL006-05.

Required Author Forms Disclosure forms provided by the authors are available with the online version of this article.

Author Contribution Y.X.T. conceived the project and supervised all the experiments. W.W., W.L., and Y.X.T. designed the project. W.W. and W.L. performed the animal model and behavioral experiments. S.D. carried out the electrophysiological recording. G.G. did the co-immunoprecipitation and Western blot experiments. W.W., W.L., S.D., G.G., A.I., A.B., and Y.X.T. analyzed the data. W.W. and Y.X.T. wrote and edited the manuscript. All of the authors read and discussed the manuscript.

Funding This work was supported by the Rutgers New Jersey Medical School start-up fund to YXT.

Declarations

Ethics Approval All procedures used were approved by the Animal Care and Use Committee at the Rutgers New Jersey Medical School (Newark, NJ, USA).

Competing Interests The authors declare no competing interests.

References

1. Mantyh PW (2006) Cancer pain and its impact on diagnosis, survival and quality of life. Nat Rev Neurosci 7: 797–809. nrn1914. https://doi.org/10.1038/nrn1914.
2. Mercadante S (1997) Malignant bone pain: pathophysiology and treatment. Pain 69: 1–18. S0304–3959(96)03267–8.
3. Grisold W, Cavaletti G, Windebank AJ (2012) Peripheral neuropathies from chemotherapeutics and targeted agents: diagnosis, treatment, and prevention. Neuro Oncol 14 Suppl 4: iv45-iv54. nos203. https://doi.org/10.1093/neuonc/nos203.
4. Windebank AJ, Grisold W (2008) Chemotherapy-induced neuropathy. J Peripher Nerv Syst 13: 27–46. JNS156. https://doi.org/10.1111/j.1529-8027.2008.00156.x.
5. Gaskin DJ, Richard P (2012) The economic costs of pain in the United States. J Pain 13: 715–724. S1526–5900(12)00559–7. https://doi.org/10.1016/j.jpain.2012.03.009.
6. Latremoliere A, Woolf CJ (2009) Central sensitization: a generator of pain hypersensitivity by central neural plasticity. J Pain 10: 895–926. S1526–5900(09)00609–9. https://doi.org/10.1016/j.jpain.2009.06.012.
7. Aiyer R, Mehta N, Gungor S, Gulati A (2018) A Systematic Review of NMDA Receptor Antagonists for Treatment of Neuropathic Pain in Clinical Practice. Clin J Pain 34: 450-467. https://doi.org/10.1097/AJP.0000000000000547.
8. Park JS, Voitenko N, Petralia RS, Guan X, Xu JT, Steinberg JP, Takamiya K, Sotnik A, Kopach O, Huganir RL, Tao YX (2009) Persistent inflammation induces GluR2 internalization via NMDA receptor-triggered PKC activation in dorsal horn neurons. J Neurosci 29: 3206–3219. 29/10/3206. https://doi.org/10.1523/JNEUROSCI.4514-08.2009.
9. Tao F, Tao YX, Gonzalez JA, Fang M, Mao P, Johns RA (2001) Knockdown of PSD-95/SAP90 delays the development of neuropathic pain in rats. Neuroreport 12: 3251-3255. https://doi.org/10.1097/00001756-200110290-00022.
10. Tao YX, Huang YZ, Mei L, Johns RA (2000) Expression of PSD-95/SAP90 is critical for N-methyl-D-aspartate receptor-mediated thermal hyperalgesia in the spinal cord. Neuroscience 98: 201–206. S0306–4522(00)00193–7 [pii];https://doi.org/10.1016/s0306-4522(00)00193-7.
11. Tao YX, Rumbaugh G, Wang GD, Petralia RS, Zhao C, Kauer FW, Tao F, Zhuo M, Wenthold RJ, Raja SN, Huganir RL, Bredt DS, Johns RA (2003) Impaired NMDA receptor-mediated postsynaptic function and blunted NMDA receptor-dependent persistent pain in mice lacking postsynaptic density-93 protein. J Neurosci 23: 6703–6712. 23/17/6703.
12. Chizh BA, Headley PM (2005) NMDA antagonists and neuropathic pain--multiple drug targets and multiple uses. Curr Pharm Des 11: 2977-2994. https://doi.org/10.2174/1381612054865082.
13. Parsons CG (2001) NMDA receptors as targets for drug action in neuropathic pain. Eur J Pharmacol 429: 71–78. S0014299901013073. https://doi.org/10.1016/s0014-2999(01)01307-3.
14. Zhou L, Li F, Xu HB, Luo CX, Wu HY, Zhu MM, Lu W, Ji X, Zhou QG, Zhu DY (2010) Treatment of cerebral ischemia by disrupting ischemia-induced interaction of nNOS with PSD-95. Nat Med 16: 1439–1443. nm.2245. https://doi.org/10.1038/nm.2245.
15. Cai W, Wu S, Pan Z, Xiao J, Li F, Cao J, Zang W, Tao YX (2018) Disrupting interaction of PSD-95 with nNOS attenuates hemorrhage-induced thalamic pain. Neuropharmacology 141: 238–248. S0028–3908(18)30618-X. https://doi.org/10.1016/j.neuropharm.2018.09.003.
16. Florio SK, Loh C, Huang SM, Iwamaye AE, Kitto KF, Fowler KW, Treiberg JA, Hayflick JS, Walker JM, Fairbanks CA, Lai Y (2009) Disruption of nNOS-PSD95 protein-protein interaction inhibits acute thermal hyperalgesia and chronic mechanical

allodynia in rodents. Br J Pharmacol 158: 494–506. BPH300. https://doi.org/10.1111/j.1476-5381.2009.00300.x.
17. Lee WH, Xu Z, Ashpole NM, Hudmon A, Kulkarni PM, Thakur GA, Lai YY, Hohmann AG (2015) Small molecule inhibitors of PSD95-nNOS protein-protein interactions as novel analgesics. Neuropharmacology 97: 464–475. S0028–3908(15)00228–2. https://doi.org/10.1016/j.neuropharm.2015.05.038.
18. Li J, Zhang L, Xu C, Lin YH, Zhang Y, Wu HY, Chang L, Zhang YD, Luo CX, Li F, Zhu DY (2020) Prolonged Use of NMDAR Antagonist Develops Analgesic Tolerance in Neuropathic Pain via Nitric Oxide Reduction-Induced GABAergic Disinhibition. Neurotherapeutics 17: 1016-1030. https://doi.org/10.1007/s13311-020-00883-w.
19. Li J, Zhang L, Xu C, Shen YY, Lin YH, Zhang Y, Wu HY, Chang L, Zhang YD, Chen R, Zhang ZP, Luo CX, Li F, Zhu DY (2021) A pain killer without analgesic tolerance designed by co-targeting PSD-95-nNOS interaction and alpha2-containning GABAARs. Theranostics 11: 5970-5985. https://doi.org/10.7150/thno.58364; thnov11p5970.
20. Chen D, Zhao T, Ni K, Dai P, Yang L, Xu Y, Li F (2016) Metabolic investigation on ZL006 for the discovery of a potent prodrug for the treatment of cerebral ischemia. Bioorg Med Chem Lett 26: 2152–2155. S0960–894X(16)30306–7. https://doi.org/10.1016/j.bmcl.2016.03.074.
21. Miao XR, Fan LC, Wu S, Mao Q, Li Z, Lutz B, Xu JT, Lu Z, Tao YX (2017) DNMT3a contributes to the development and maintenance of bone cancer pain by silencing Kv1.2 expression in spinal cord dorsal horn. Mol Pain 13: 1744806917740681. https://doi.org/10.1177/1744806917740681.
22. Schwei MJ, Honore P, Rogers SD, Salak-Johnson JL, Finke MP, Ramnaraine ML, Clohisy DR, Mantyh PW (1999) Neurochemical and cellular reorganization of the spinal cord in a murine model of bone cancer pain. J Neurosci 19: 10886-10897.
23. Zhang RX, Liu B, Wang L, Ren K, Qiao JT, Berman BM, Lao L (2005) Spinal glial activation in a new rat model of bone cancer pain produced by prostate cancer cell inoculation of the tibia. Pain 118: 125–136. S0304–3959(05)00383–0. https://doi.org/10.1016/j.pain.2005.08.001.
24. Mao Q, Wu S, Gu X, Du S, Mo K, Sun L, Cao J, Bekker A, Chen L, Tao YX (2019) DNMT3a-triggered downregulation of K2p 1.1 gene in primary sensory neurons contributes to paclitaxel-induced neuropathic pain. Int J Cancer. https://doi.org/10.1002/ijc.32155.
25. Yang Y, Wen J, Zheng B, Wu S, Mao Q, Liang L, Li Z, Bachmann T, Bekker A, Tao YX (2021) CREB Participates in Paclitaxel-Induced Neuropathic Pain Genesis Through Transcriptional Activation of Dnmt3a in Primary Sensory Neurons. Neurotherapeutics 18: 586-600. https://doi.org/10.1007/s13311-020-00931-5.
26. Fu G, Du S, Huang T, Cao M, Feng X, Wu S, Albik S, Bekker A, Tao YX (2021) FTO (Fat-Mass and Obesity-Associated Protein) Participates in Hemorrhage-Induced Thalamic Pain by Stabilizing Toll-Like Receptor 4 Expression in Thalamic Neurons. Stroke 52: 2393-2403. https://doi.org/10.1161/STROKEAHA.121.034173.
27. Pan Z, Du S, Wang K, Guo X, Mao Q, Feng X, Huang L, Wu S, Hou B, Chang YJ, Liu T, Chen T, Li H, Bachmann T, Bekker A, Hu H, Tao YX (2021) Downregulation of a Dorsal Root Ganglion-Specifically Enriched Long Noncoding RNA is Required for Neuropathic Pain by Negatively Regulating RALY-Triggered Ehmt2 Expression. Adv Sci (Weinh) 8: e2004515. https://doi.org/10.1002/advs.202004515.
28. Grenald SA, Doyle TM, Zhang H, Slosky LM, Chen Z, Largent-Milnes TM, Spiegel S, Vanderah TW, Salvemini D (2017) Targeting the S1P/S1PR1 axis mitigates cancer-induced bone pain and neuroinflammation. Pain 158: 1733-1742. https://doi.org/10.1097/j.pain.0000000000000965.
29. Li Y, Guo X, Sun L, Xiao J, Su S, Du S, Li Z, Wu S, Liu W, Mo K, Xia S, Chang YJ, Denis D, Tao YX (2020) N(6)-Methyladenosine Demethylase FTO Contributes to Neuropathic Pain by Stabilizing G9a Expression in Primary Sensory Neurons. Adv Sci (Weinh) 7: 1902402. https://doi.org/10.1002/advs.201902402; ADVS1771.
30. Zhao JY, Liang L, Gu X, Li Z, Wu S, Sun L, Atianjoh FE, Feng J, Mo K, Jia S, Lutz BM, Bekker A, Nestler EJ, Tao YX (2017) DNA methyltransferase DNMT3a contributes to neuropathic pain by repressing Kcna2 in primary afferent neurons. Nat Commun 8: 14712. ncomms14712. https://doi.org/10.1038/ncomms14712.
31. Zhao X, Tang Z, Zhang H, Atianjoh FE, Zhao JY, Liang L, Wang W, Guan X, Kao SC, Tiwari V, Gao YJ, Hoffman PN, Cui H, Li M, Dong X, Tao YX (2013) A long noncoding RNA contributes to neuropathic pain by silencing Kcna2 in primary afferent neurons. Nat Neurosci 16: 1024–1031. nn.3438. https://doi.org/10.1038/nn.3438.
32. Carey LM, Lee WH, Gutierrez T, Kulkarni PM, Thakur GA, Lai YY, Hohmann AG (2017) Small molecule inhibitors of PSD95-nNOS protein-protein interactions suppress formalin-evoked Fos protein expression and nociceptive behavior in rats. Neuroscience 349: 303–317. S0306–4522(17)30146-X. https://doi.org/10.1016/j.neuroscience.2017.02.055.